

Experimental Study of Electron Vortex Structures in an Electrostatic Plasma Lens

Yu. N. Chekh

Institute of Physics, National Academy of Sciences of Ukraine, pr. Nauki 46, Kiev, 03680 Ukraine

Received July 23, 2007

Abstract—Results are presented from experimental studies of electron vortex bunches in a cold ion-beam plasma consisting of strongly magnetized electrons and a beam of almost free positive ions. The existence of electron vortex bunches was detected from local minima of the electric potential on surfaces perpendicular to the magnetic field lines. It is found that the vortices have the form of magnetic-field-aligned filaments, in which electrons rotate with a velocity significantly exceeding both the velocity of the vortex as a whole and the electron velocity in the ambient plasma. It is shown that, in a sufficiently strong magnetic field, the accumulation of electrons in the vortices terminates when the condition for the longitudinal confinement of electrons by the electric field fails to hold.

PACS numbers: 52.25.Xz, 52.27.Jt, 52.35.-g, 52.35.Fp, 52.35.Kt, 52.35.We, 52.35.Mw

DOI: 10.1134/S1063780X08050097

1. INTRODUCTION

It is known (see, e.g., [1, 2]) that vortices can significantly affect the static and dynamical parameters of the system in which they develop. In particular, the formation of electron vortices can drastically alter the parameters of plasma-dynamic devices. Since plasma vortices are rather difficult to investigate experimentally, most studies in this field, especially those concerning multi-component plasmas, are theoretical.

This paper presents results from experimental studies of the possibility of vortex formation in an ion-beam plasma consisting of magnetized electrons and a high-current beam of unmagnetized positive ions. Such conditions are typical of various plasma-dynamic (in particular, plasma-optical) devices [3]. One such device is the electrostatic plasma lens (PL) [3–5].

For the first time, the formation of electron vortices in a PL was observed in the experimental work [6], which was based on the results of theoretical studies [7, 8].

2. THEORETICAL ANALYSIS OF THE MEDIUM DYNAMICS IN A PLASMA LENS

The possibility of vortex formation in a PL was demonstrated in numerical simulations [7] of a magnetized electron column whose space charge was partially neutralized by a static ion background. In [8], the formation of electron vortices was also considered analytically with allowance for ion motion in the linear approximation. In both cases, the initial distribution of electrons was assumed to be uniform and only the mag-

netic-field gradient was taken into account. Here, we consider the opposite case where the initial electron-density gradient is large enough for the magnetic-field gradient can be ignored.

We introduce a cylindrical coordinate system with the z axis directed along the magnetic field. The plasma is assumed to be uniform along the z axis. The basic equations describing the two-dimensional dynamics of strongly magnetized cold electrons ($\omega_e \ll \omega_{ce}$) have the form

$$\nabla\varphi = [\mathbf{v} \times \mathbf{B}], \quad (1)$$

$$\frac{\partial n_e}{\partial t} + (\mathbf{v} \cdot \nabla)n_e = 0, \quad (2)$$

$$\Delta\varphi = e(n_e - Zn_i)/\epsilon_0, \quad (3)$$

where $\omega_e = (en_e/\epsilon_0 m)^{1/2}$ is the electron Langmuir frequency, $\omega_{ce} = eB/m$ is the electron cyclotron frequency, e and m are the charge and mass of an electron, \mathbf{v} is the electron velocity, n_e is the electron density, n_i is the ion density, φ is the electric potential, B is the magnetic induction, Z is the ion charge number, and ϵ_0 is the permittivity of vacuum. The set of Eqs. (1)–(3) yields the following nonlinear equation describing the dynamics of a charged plasma in a general case, irrespectively of the type of ion dynamics:

$$\frac{\partial}{\partial t} \left(\Delta\varphi + \frac{Ze}{\epsilon_0} n_i \right) + \frac{J(\varphi, \Delta\varphi)}{rB} + \frac{Ze}{\epsilon_0} \mathbf{v} \nabla n_i = 0, \quad (4)$$

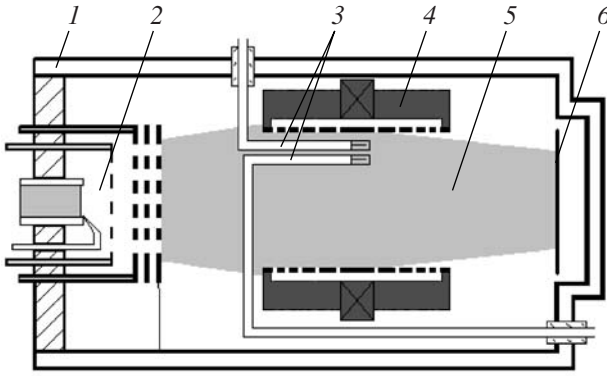


Fig. 1. Schematic of the experimental setup: (1) vacuum chamber, (2) ion source, (3) capacitive or Langmuir probes, (4) PL, (5) ion beam, and (6) collector.

where $J(a, b) = \frac{\partial a \partial a}{\partial r \partial \theta} - \frac{\partial a \partial b}{\partial \theta \partial r}$ is the Jacobian. Thus, the possibility of vortex formation is determined by the presence of vector nonlinearity.

It follows from Eqs. (1) and (3) that the vorticity α (the longitudinal component of the curl of the electron velocity) is proportional to the space charge density ρ (see also [8, 9]):

$$\alpha = \rho / \varepsilon_0 B. \quad (5)$$

Evidently, the condition $\alpha \neq 0$ does not necessarily imply the formation of a vortex, because the vortex should contain trapped particles whose rotation velocity is much larger than the velocity of the structure as a whole [10]. To ensure particle trapping in the transverse plane, the parameter α and, accordingly, ρ should be sufficiently large.

Let us consider the case where local regions with enhanced values of ρ form due to the onset of azimuthal electron-ion instability in crossed electric and magnetic fields in the presence of an electron-density gradient. The linear stage of this instability in a plane geometry is described by an equation derived in [11] with allowance for both the magnetic-field and electron-density gradients. In the absence of a radial magnetic-field gradient, this equation in cylindrical coordinates has the form

$$1 - \frac{\omega_{i0}^2}{\omega^2} - \frac{\omega_{e0}^2 \partial n_{e0} / \partial r}{n_{e0} (l_\theta / r) \omega_{ce} (\omega - l_\theta \omega_{\theta 0})} = 0, \quad (6)$$

where ω is the frequency of perturbations; ω_{i0} and ω_{e0} are the unperturbed ion and electron Langmuir frequencies, respectively; $\omega_{\theta 0}$ is the unperturbed velocity of electron rotation around the system axis due to the drift in crossed electric and magnetic fields; and l_θ is the azimuthal mode number. Note that this equation can also

be obtained by linearizing Eq. (4) and explicitly taking into account the ion dynamics:

$$n_i' = -(Ze/M)n_{i0}\Delta\phi/\omega^2,$$

where M is the mass of an ion. Hereafter, the zero subscript and prime refer to unperturbed and perturbed quantities, respectively.

If $\omega \ll l_\theta \omega_{\theta 0}$ and $\partial n_{e0} / \partial r < 0$, then Eq. (6) has a solution with the maximal growth rate $\gamma_{\max} = \sqrt{3} \omega$ at

$$\omega = \frac{1}{2} (\omega_{\theta 0} \omega_{i0}^2 l_\theta)^{1/3} = \frac{1}{2} \left(-\frac{\omega_{e0}^2 \omega_{i0}^2}{(l_\theta / r) \omega_{ce} n_{e0}} \frac{\partial n_{e0}}{\partial r} \right)^{1/3}.$$

This instability is related to the excitation of beam ion oscillations by the electron gradient wave propagating in the azimuthal direction. When the amplitude of this wave becomes large enough, a chain of electron vortices can form in the lens.

Note that, for this instability to be efficiently excited, the following condition determined by the drift of perturbations in the beam propagation direction should also be satisfied [11]:

$$\gamma > u_{ib} / L, \quad (7)$$

where γ is the instability growth rate, u_{ib} is the beam ion velocity, and L is the length of the lens. Using the equality $\gamma = \sqrt{3} \omega$; setting $L \approx R_L$ (where R_L is the lens radius); and taking into account that, under the given experimental conditions, $\omega \sim \omega_{i0}$, we obtain from Eq. (7) the approximate formula

$$I_b / \varphi_{\text{acc}}^{3/2} > 3 \varepsilon_0 (Ze/M)^{1/2}, \quad (8)$$

where φ_{acc} is the beam accelerating voltage and I_b is the beam current.

Let us consider a characteristic feature indicating vortex formation. In the transverse cross section of the vortex, the electron trajectories must be closed. Since, according to Eq. (1), the electrons move along equipotential surfaces [4] and the electron trajectories should be closed in the transverse cross section of the vortex, the electric potential should have extrema in a surface perpendicular to the magnetic field lines. Simple geometric considerations show that, if all the vortices rotate in the same azimuthal direction, such extrema should correspond to local minima (maxima) in the distribution of the minimum (maximum) values of the potential measured along a curve whose tangent is perpendicular to the magnetic field lines. The local maxima correspond to electron vortex cavities, which are dominated by the positive space charge ($\rho > 0$), while the local minima correspond to electron vortex bunches, in which $\rho < 0$.

3. EXPERIMENTAL SETUP AND DIAGNOSTIC TECHNIQUES

High-current pulsed-periodic ion beam was produced by a wide-aperture vacuum-arc source [12], passed through the PL, and then arrived at a metal collector (Fig. 1). The beam pulse duration was 100 μ s, the pulse repetition rate was 0.5 Hz, the initial beam diameter was 6 cm, the beam current was $I_b = 50\text{--}600$ mA, and the accelerating voltage was $\phi_{\text{acc}} = 6\text{--}24$ kV. The experiments were performed with copper, carbon, and lead ion beams. The ion density n_i in the beam was calculated from the beam current and was typically about 10^{14} m $^{-3}$. The residual gas pressure was less than 2×10^{-5} Torr.

The PL schematic is shown in Fig. 2. The PL electrodes were wide metal rings arranged with a small gap (~ 1 mm) along the lens axis. The inner radius of the electrodes was $R_L = 37$ mm. The magnetic field was produced by permanent magnets. At the center of the lens, the magnetic induction was 36–41 mT. The electrodes were connected pairwise, symmetrically with respect to the central electrode. The maximum positive voltage ϕ_L (up to 3 kV) was applied to the central and several neighboring electrodes, whereas the other electrodes were grounded. The electrode system was supplied from a dc or a pulsed voltage source. In the latter case, a fraction of the pulsed accelerating voltage of the ion source was supplied to the PL electrodes through a resistive divider. The experiments were performed with different schemes of voltage supply to the PL electrodes: the voltage was applied to the central electrode and one, two, or three neighboring pairs of electrodes (below, these schemes are conventionally denoted as an SPD, MPD, and LPD scheme, respectively).

The azimuthal and radial distributions of the electric potential and electric field in the lens were measured by cylindrical Langmuir and capacitive probes. The diameter and length of the sensitive part of a capacitive probe were 1 and 8 mm, respectively. The azimuthal profile of the potential of the excited waves was determined using the waveforms of the probe signals. The azimuthal velocity of the waves was calculated from the phase shift of the oscillations recorded by two azimuthally spaced probes. The transmission gain of the measurement circuits differed by no more than $\approx 10\%$ in the frequency range from 10 kHz to 15 MHz. All the probes were aligned along the PL axis. In what follows (unless otherwise specified), it is implied that the sensitive parts of the probes are located in the central cross section of the lens. The signals were recorded by an S8-14 oscilloscope with a passband of 50 MHz and an ASK-3151 digital oscilloscope adapter.

4. EXPERIMENTAL RESULTS AND DISCUSSION

Numerical simulations [13] showed that dense electron layers can form in a PL. These layers are generated due to ion-induced electron emission from the PL elec-

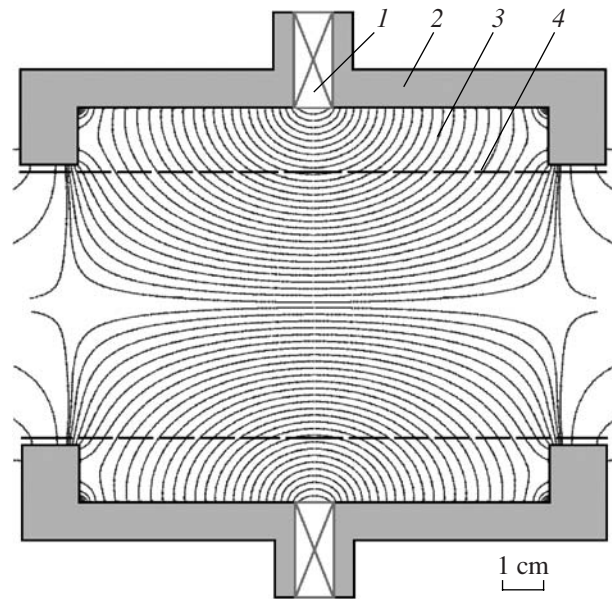


Fig. 2. Schematic of an axially symmetric PL: (1) permanent magnets, (2) magnetic core, (3) magnetic field lines, and (4) electrodes.

trodes, which are bombarded by the peripheral ions of the ion beam propagating through the lens. Since the magnetic field lines are equipotential and since the plasma and the electrodes can exchange electrons, the layers form near the field lines that pass through the gaps between the cylindrical fixing electrodes, thereby ensuring the transfer of the stepwise distribution of the potential over the electrodes into the lens volume. The existence of a region with a negative gradient of the electron density can cause the onset of the above instability. In this paper, a single dense electron layer was formed by applying a large potential difference to the neighboring pairs of electrodes.

Let us consider the experimental results demonstrating the onset of instability and the generation of waves of the electric potential, looking aside for a moment from the vortex nature of perturbations. Figures 3 and 4 show typical dependences of the parameters of the observed azimuthal waves on the lens voltage and beam current. It can be seen that the oscillation frequency is approximately equal to the ion Langmuir frequency, the mode number is inversely proportional to the voltage supplied to the PL electrodes, and the phase velocity (which is proportional to v/l_0) increases nearly linearly with increasing electrode voltage. It should be noted that lower mode numbers correspond to waves with lower frequencies and phase velocities.

Under our experimental conditions, the threshold character of the instability (see inequality (8)) is much more pronounced than in [11]. According to inequality (8), the threshold current is about 200 mA for a C $^{+}$ beam and $\phi_{\text{acc}} = 18$ kV. This agrees well with the exper-

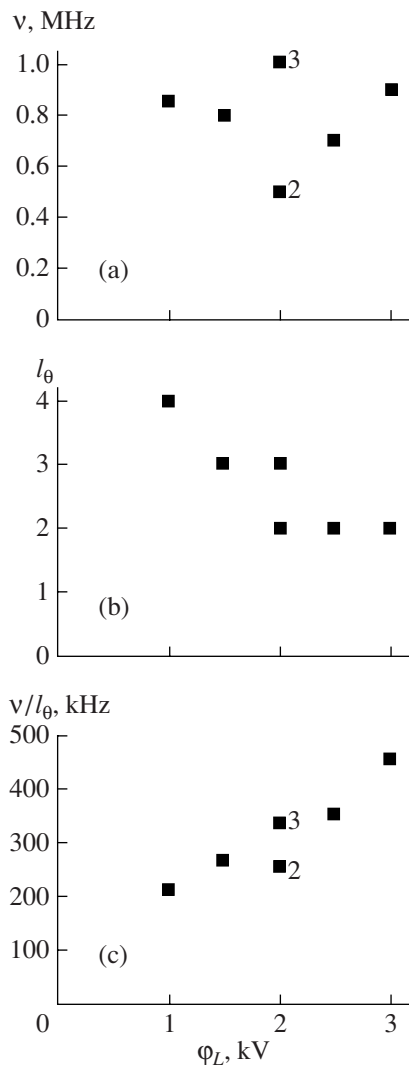


Fig. 3. (a) Frequency v , (b) mode number l_θ , and (c) ratio v/l_θ as functions of the lens voltage (LPD scheme, copper ion beam, $\phi_{acc} = 6$ kV, and $I_b = 80$ mA). The numerals by the squares indicate the mode number.

imentally observed value of the threshold current (Fig. 5). A tendency toward the suppression of instability was also observed for a copper ion beam at $\phi_{acc} = 24$ kV and $I_b \approx 200$ mA.

The observed waves of the electric potential are strongly nonlinear because their amplitude is close to the potential applied to the PL electrodes (Fig. 6). Note that the spatial region in which the wave amplitude is maximum almost coincides with the position of the drop in the potential distribution defined by the scheme of voltage supply to the PL electrodes. For the narrow potential distribution (SPD scheme), the maximum of the wave amplitude is located closer to the central electrode than in the case of the wide distribution (LPD scheme).

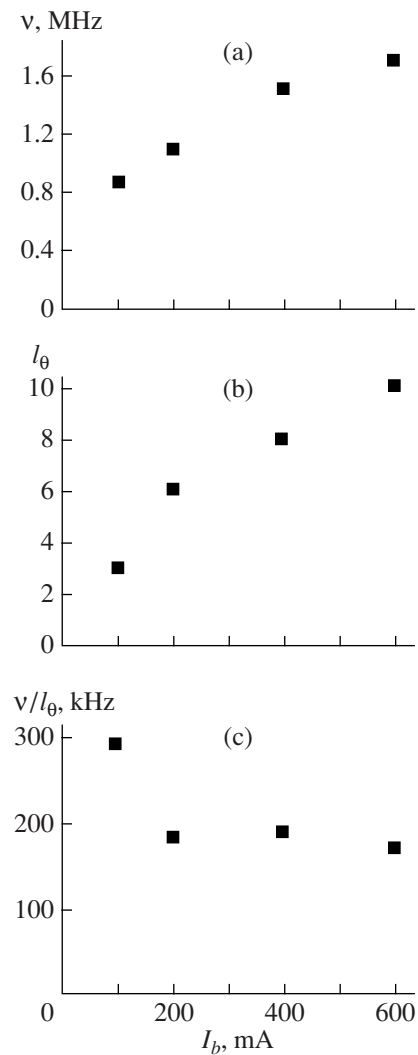


Fig. 4. (a) Frequency v , (b) mode number l_θ , and (c) ratio v/l_θ as functions of the beam current (MPD scheme, carbon ion beam, $\phi_L = 1$ kV, $B = 41$ mT, and $\phi_{acc} = 18$ kV).

It was found that only local minima of the electric potential form in the central cross section of the lens due to the onset of instability (Fig. 7). The formation of such local minima can be seen in the oscilloscope traces shown in Fig. 8. Thus, the observed waves of the electric potential indicate the generation of electron vortex bunches, the mode number l_θ being equal to the number of vortices in a chain. By measuring the characteristic vortex size and the value of the electric field in a vortex, we can roughly estimate the frequency of electron rotation in the vortices. This frequency turns out to be a few tens of megahertz, which agrees satisfactorily with the frequency of small-scale oscillations observed in the minima of the electric potential [6].

The oscilloscope traces presented in Fig. 8 show that the accumulation of electrons in the vortices terminates when the condition for the longitudinal confinement of

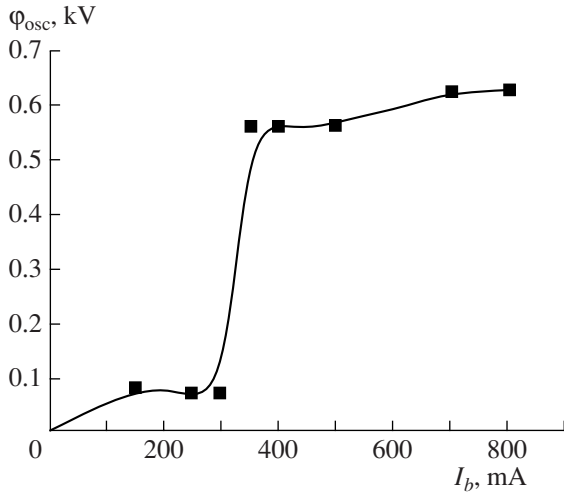


Fig. 5. Amplitude of oscillations of the electric potential in the lens vs. beam current (SPD scheme, carbon ion beam, $\varphi_L = 0.9$ kV, $B = 41$ mT, and $\varphi_{acc} = 18$ kV).

electrons in the lens fails to hold, so that the electrons can freely escape to the electrodes along the magnetic field lines. It is clearly seen in Fig. 8c that the potential does not decrease below the potential of the electrode that is crossed by the field lines passing through the vortex (in the case at hand, this potential is zero). A more detailed examination shows that in some (fairly rare) cases, the potential can decrease below zero, but the absolute value of the resulting negative potential does not exceed $T_e/e \sim 10$ V, where T_e is the characteristic electron temperature. The time interval during which the potential is negative is about 0.1 μ s, which is

approximately equal to the time of flight of thermal electrons along the field line.

Figure 9 shows the spatial distributions of the parameters of electric potential oscillations within the lens (note that only two of these parameters are independent), measured with a step of 5 mm. These distributions also indicate that only local minima corresponding to electron vortex bunches form in the lens. The shaded region in Fig. 9b shows the positions of these vortices which, as was expected, are stretched along the magnetic field lines. The gap in the structure is presumably related to the fact that the vortex axis in this region is inclined by a fairly large angle with respect to the axial direction, along which the probe is oriented; this manifests itself as an apparent increase in the electric potential.

Let us consider the structure shown in Fig. 9c. The configuration of the equipotential lines in this region differs substantially from that of the magnetic field lines. In this case, the assumption that the electrons move along equipotential surfaces is invalid. The electrons propagating through such a structure gain a fairly large energy due to the acceleration in the magnetic-field-aligned electric field. Therefore, in order to adequately describe electron motion in this region, it is necessary to take into account both the longitudinal component of the electric field and electron inertia.

The fact that only vortex bunches form in the lens can be ascribed to permanent electron emission from the electrode surfaces bombarded by the beam ions. The injection of such electrons can intensify vortex bunches and suppress vortex cavities.

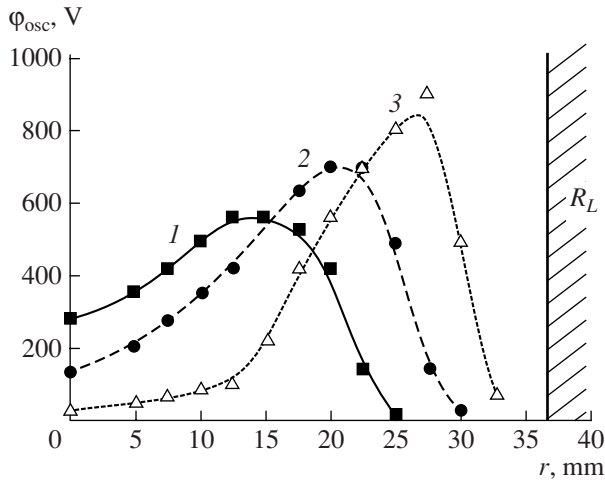


Fig. 6. Radial profile of the maximum amplitude of oscillations of the electric potential in the central cross section of the lens (copper ion beam, $B = 41$ mT, $\varphi_{acc} = 12$ kV, $\varphi_L = 1$ kV, and $I_b = 400$ mA) for different schemes of voltage supply to the lens electrodes: (1) LPD, (2) MPD, and (3) SPD.

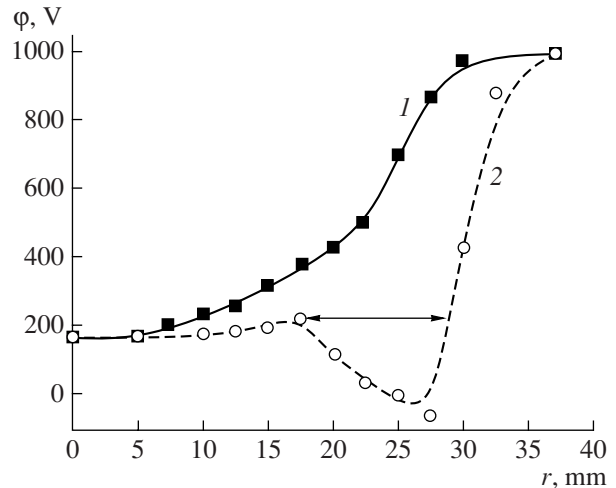


Fig. 7. Radial distributions of the (1) maximum and (2) minimum values of the potential in the central cross section of the lens (SPD scheme, copper ion beam, $\varphi_L = 1$ kV, $B = 41$ mT, $\varphi_{acc} = 12$ kV, and $I_b = 400$ mA). The radial size of the vortex is indicated by the double-headed arrow.

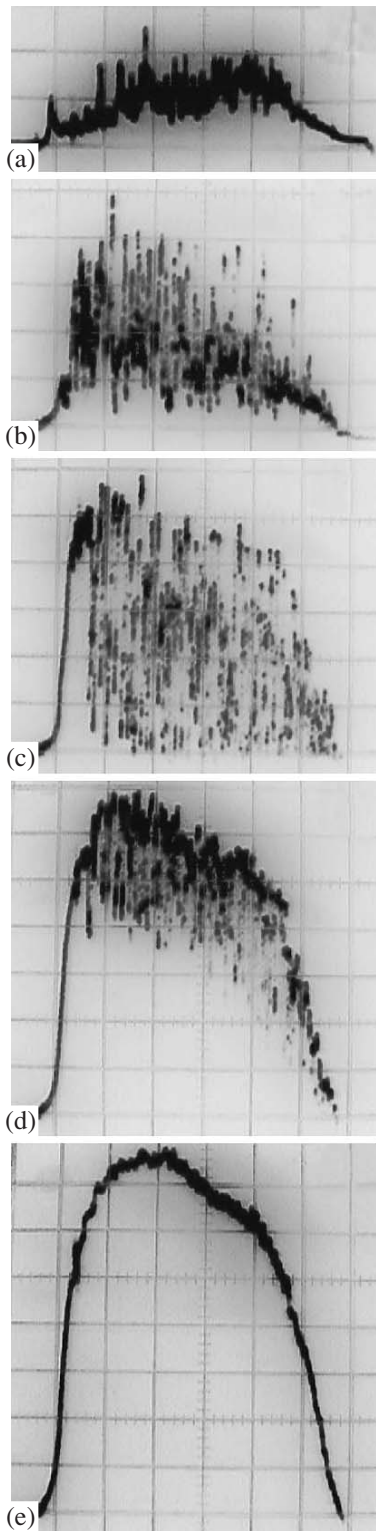


Fig. 8. Oscilloscope traces of the electric potential in the central cross section of the lens at different distances from the lens axis in the case of a pulsed voltage supply to the electrodes (SPD scheme, copper ion beam, $\varphi_L = 1$ kV, $B = 41$ mT, $\varphi_{acc} = 24$ kV, and $I_b = 150$ mA): $r =$ (a) 0, (b) 20, (c) 25, (d) 30, and (e) 35 mm. The voltage scale is 135 V/div, and the time scale is 20 μ s/div.

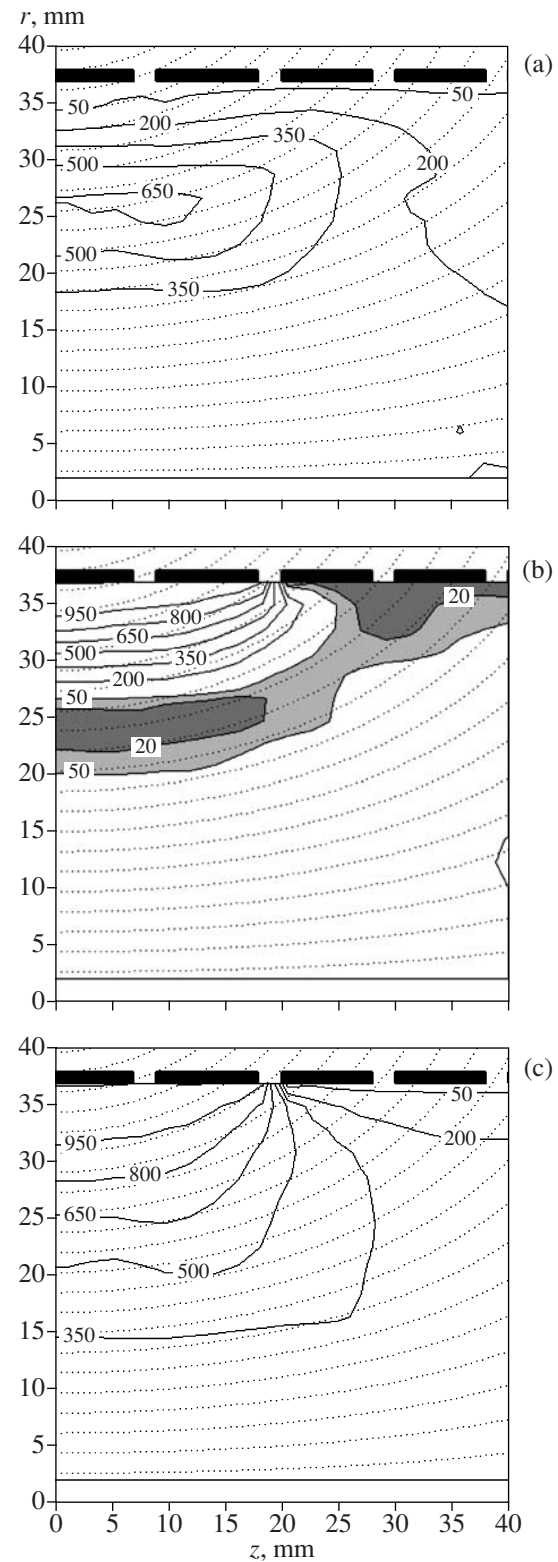


Fig. 9. Spatial distributions of the parameters of electric potential oscillations within the lens, averaged over several pulses: (a) oscillation amplitude, (b) minimum value of the potential, and (c) maximum value of the potential. The magnetic field lines are shown by dotted curves. The experimental conditions are the same as in Fig. 8.

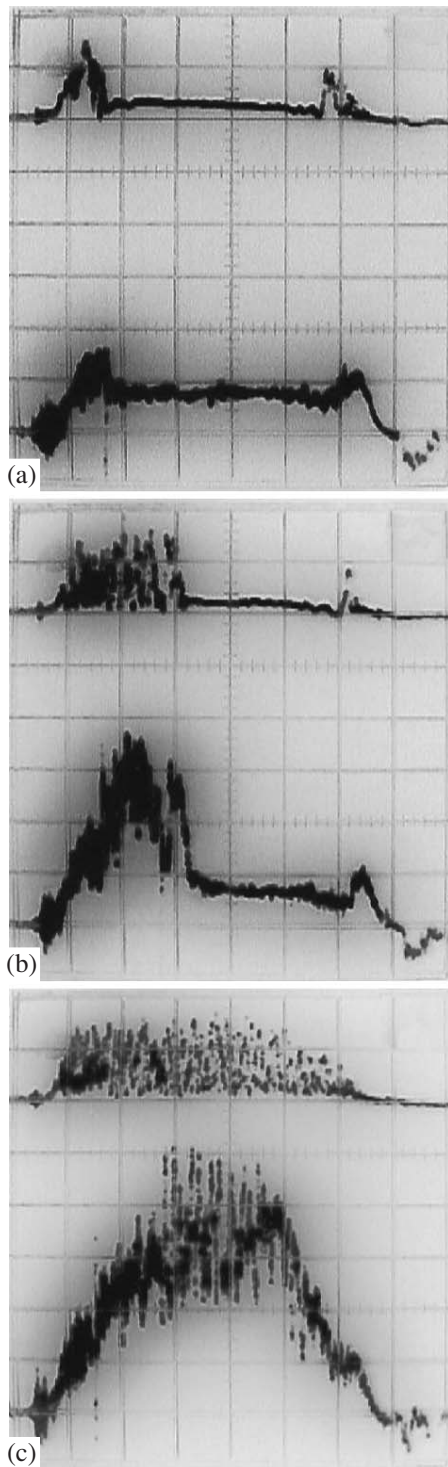


Fig. 10. Oscilloscope traces of the electric potential in the central cross section of the lens (upper trace) and the current in the ground circuit of the lens electrodes (lower trace) (SPD scheme, copper ion beam, $\phi_L = 1$ kV, $B = 41$ mT, and $\phi_{acc} = 24$ kV). The beam current, $I_b \approx 200$ mA, is close to the threshold value for the onset of instability (see Eq. (8)). The difference in the plasma dynamics in panels (a)–(c) is caused only by small random pulse-to-pulse variations in the beam current. The voltage scale is 540 V/div, and the current scale is 60 mA/div.

To conclude, we note that the presence of a sharp threshold for the onset of instability can be used to compare the electron currents collected from the regions adjacent to the grounded electrodes under conditions where the instability is absent and where vortices are generated, all other conditions being the same. It can be seen in Fig. 10 that, in the latter case, the currents in the ground circuits of these electrodes increase by almost one order of magnitude; i.e., the leakage currents of electrons across the magnetic field onto the electrodes that are at the maximum potential increase multifold.

5. CONCLUSIONS

Thus, the results obtained in this study show that, in the presence of a negative radial gradient of the electron density in a PL, the azimuthal flow of magnetized electrons amplifies ion oscillations in the ion beam propagating through the lens. The onset of instability leads to the amplification of azimuthal waves of the electric potential at frequencies close to the ion plasma frequency. As the wave amplitude increases, the vector nonlinearity results in the trapping of electrons and the formation of a chain of electron vortex bunches dominated by the electron space charge. The electrons in the vortex rotate along closed trajectories perpendicular to the magnetic field lines. The velocity of this rotation is much higher than both the rotation velocity of the vortex as a whole and the velocity at which untrapped electrons rotate around the lens axis. Due to the high electron mobility, the vortices stretch along the magnetic field lines and vortex filaments form. In the strong magnetic field used in our experiments, the accumulation of electrons in the vortices terminates when the space charge density reaches the value at which the electric potential within the vortex becomes equal to the potential of the surface that is crossed by the magnetic field lines passing through the vortex, i.e., when the condition for the longitudinal confinement of electrons by the electric field fails to hold. The formation of vortices leads to a significant increase in the leakage currents of electrons across the magnetic field lines.

ACKNOWLEDGMENTS

The author is grateful to Prof. A.A. Goncharov for his help in all the stages of this work.

REFERENCES

1. J. J. Rasmussen, J. P. Lynov, J. S. Hesthaven, and G. G. Sutyurin, *Plasma Phys. Controlled Fusion* **36**, B193 (1994).
2. W. Horton, B. Hu, J. D. Dong, and P. Zhu, *New J. Phys.* **5**, 14.1 (2003).
3. A. I. Morozov, *Introduction to Plasmodynamics* (Fizmatlit, Moscow, 2006) [in Russian].

4. A. I. Morozov and S. V. Lebedev, *Reviews of Plasma Physics*, Ed. by M. A. Leontovich (Atomizdat, Moscow, 1974; Consultants Bureau, New York, 1980), Vol. 8.
5. A. Goncharov, *Handbook of Ion Sources*, Ed. by B. H. Wolf (CRC, New York, 1995), p. 379.
6. Yu. N. Chekh, A. A. Goncharov, and I. M. Protsenko, *Pis'ma Zh. Tekh. Fiz.* **32** (2), 8 (2006) [*Tech. Phys. Lett.* **32**, 51 (2006)].
7. A. Goncharov and I. Litovko, *IEEE Trans. Plasma Sci.* **27**, 1073 (1999).
8. A. A. Goncharov, V. I. Maslov, and I. N. Onishchenko, *Fiz. Plazmy* **30**, 713 (2004) [*Plasma Phys. Rep.* **30**, 662 (2004)].
9. C. F. Driscoll, D. Z. Jin, D. A. Schecter, and D. H. E. Dubin, *Physica C* **369**, 21 (2002).
10. M. V. Nezlin and G. P. Chernikov, *Fiz. Plazmy* **21**, 975 (1995) [*Plasma Phys. Rep.* **21**, 922 (1995)].
11. A. A. Goncharov, A. N. Dobrovolskiĭ, A. N. Kotsarenko, et al., *Fiz. Plazmy* **20**, 499 (1994).
12. I. G. Brown, *Rev. Sci. Instrum.* **65**, 3061 (1994).
13. V. N. Gorshkov, A. A. Goncharov, and A. M. Zavalov, *Fiz. Plazmy* **29**, 939 (2003) [*Plasma Phys. Rep.* **29**, 874 (2003)].

Translated by A.V. Serber

Copyright of Plasma Physics Reports is the property of Springer Science & Business Media B.V. and its content may not be copied or emailed to multiple sites or posted to a listserv without the copyright holder's express written permission. However, users may print, download, or email articles for individual use.